



Molecular characterization of disinfection byproduct precursors in filter backwash water from 10 drinking water treatment plants

Yunkun Qian ^a, Yijun Shi ^a, Jun Guo ^a, Yanan Chen ^a, David Hanigan ^b, Dong An ^{a,c,*}

^a Department of Environmental Science & Engineering, Fudan University, Shanghai 200238, PR China

^b Department of Civil and Environmental Engineering, University of Nevada, Reno, NV 89557-0258, USA

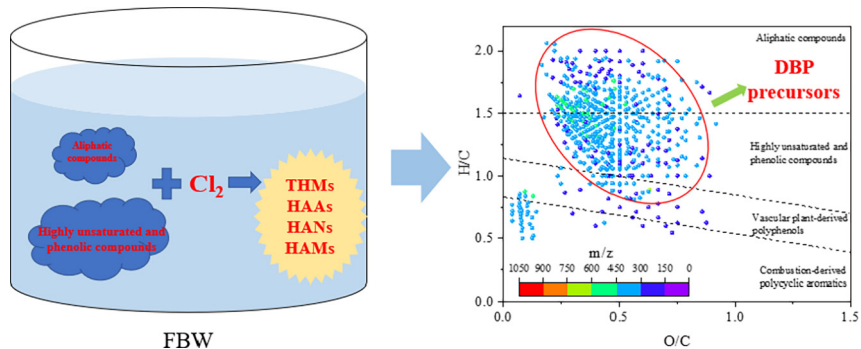
^c Shanghai Institute of Pollution Control and Ecological Security, Shanghai 200092, PR China



HIGHLIGHTS

- Low MW (<1 kDa) organic matter contributed the greatest to DBP formation.
- Aromatic and oxidized compounds were highly reactive with chlorine.
- THM, HAN, and HAM FPs were correlated with low MW aliphatic and phenolic compounds.
- HAA FP was correlated with low MW, highly unsaturated and phenolic compounds.

GRAPHICAL ABSTRACT



ARTICLE INFO

Editor: Damia Barcelo

Keywords:

FT-ICR-MS
Haloacetonitriles
Haloacetamides
Molecular characteristics
Nontarget analysis

ABSTRACT

Organic matter reacts with chlorine forming disinfection byproducts (DBPs) including trihalomethanes (THMs), haloacetamides (HAMS), haloacetic acids (HAAs), and haloacetonitriles (HANs). Filter backwash water (FBW) is either released back to the environment or recycled to the head of the treatment plant after solids settling and the remaining dissolved organic matter is a significant pool of DBP precursors that are not well understood. We characterized dissolved organic matter in FBW from 10 treatment plants and low molecular weight (MW < 1 kDa) organic matter contributed the most to DBP formation. We demonstrated overall similarity of the molecular composition (e.g., elemental ratios, m/z , DBE) of the 10 samples of FBW by Fourier transform ion cyclotron resonance mass spectrometry. Aromatic and more highly oxidized compounds preferentially reacted with chlorine, forming DBPs. Low MW (<450 Da) aliphatic compounds, and highly unsaturated and phenolic compounds were the primary precursors of THMs, HANs, and HAMs, and the formation potentials (FPs) of these groups of DBPs were correlated with multiple individual molecular formulae. HAA FPs were correlated with low MW, highly unsaturated and phenolic compounds. These advances in the understanding of the molecular composition of DBP precursors in FBW may develop the effective strategies to control DBP formation and limit impacts on the quality of finished water, and can be expanded to understanding DBP precursors in drinking water sources.

1. Introduction

* Corresponding author at: Department of Environmental Science & Engineering, Fudan University, Shanghai 200238, PR China.

E-mail address: andong@fudan.edu.cn (D. An).

Environment pollution and social development have exacerbated the shortage of global water resources and clean water supplies

(Baldassarre et al., 2018; Kummu et al., 2010; Yang et al., 2015). Reducing the discharge of produced wastewater is an effective method to control water pollution and improves drinking water production efficiency at drinking water treatment plants (DWTPs) (L. Li et al., 2018). Discharge produced by DWTPs includes sedimentation sludge water (SSW) and filter backwash water (FBW), of which FBW water accounts for approximately 1–5 % of total DWTP water flow (Gottfried et al., 2008; Shafiquzzaman et al., 2018). In China, FBW is usually discharged to surface water after being treated by sedimentation. In the U.S., FBW is typically subjected to sedimentation and the supernatant is recycled to the head of the DWTP and blended with raw water. In the future, FBW can be recycled to the head of the DWTP in China. Although recycling FBW improves water use efficiency and sedimentation of FBW removes suspended solids well, dissolved organic matter (DOM) is poorly removed. Thus, some specific organic matter originating in FBW contributes to DWTP intake DOM either through release to surface water and downstream uptake by a DWTP, or through in-plant recycling.

Drinking water disinfectants react with DOM to form disinfection byproducts (DBPs), and >700 DBPs have been identified in tap water, finished water, etc. (Krasner et al., 2018; Richardson et al., 2007; Szczuka et al., 2017). Among them, trihalomethanes (THMs) and haloacetic acids (HAAs) tend to form at the greatest mass concentrations and have been regulated in many countries (Chuang et al., 2019; Plewa et al., 2010). Thus, there is a significant amount of published research on the occurrence, formation and precursor characteristics of THMs and HAAs. However, nitrogenous DBPs (N-DBPs, e.g., haloacetamides (HAMS) and haloacetonitriles (HANs)) are significantly more cyto- and genotoxic than carbonaceous DBPs (Plewa et al., 2002, 2008; Wagner and Plewa, 2017) and the characteristics of their precursors are not as well understood, particularly those precursors present in FBW.

One study has demonstrated that recycling FBW increases DBP precursor loading; the recycled organic matter accounted for 8–31 % of the THM and HAA precursor loading in the finished water (Walsh et al., 2008). Additionally, we have shown that large quantities of THM, HAA, HAM, and HAN precursors are present in FBW (Qian et al., 2021) and that low molecular weight (MW) and hydrophilic DOM is the primary source of the precursors (Hu et al., 2021; Qian et al., 2020). While these studies provide a coarse understanding of the characteristics of precursors in FBW and demonstrate that they contribute to finished water DBP precursor loading, there is little known about the molecular characteristics of FBW-associated precursors. A better understanding of FBW-associated precursors may inform opportunities for their removal or chemical inactivation.

One technique which has been applied to characterize low MW organic matter is Fourier transform ion cyclotron resonance mass spectrometry (FT-ICR-MS) (Chen et al., 2020; Maizel et al., 2017). Organic matter is measured as individual *m/z* ratios and formulae and elemental composition (e.g., CHO, CHOS, CHON, and CHOCl, etc.) can be identified (Smith et al., 2018). Several studies have even established correlations between individual molecular formulae and DBP formation potential (FP) (Hanigan et al., 2022; Sanchís et al., 2021; Spencer et al., 2014). It has also been demonstrated that DOM with high O/C ratios contribute substantially to the formation of THMs and HAAs in source water (Wang et al., 2017). Other researchers found that more saturated compounds were primary *N*-nitrosodimethylamine (NDMA) precursors in several natural reservoirs (Farre et al., 2019; Sanchís et al., 2020, 2021). Such improvements in our understanding of the DBP precursor pool are crucial to engineering solutions which remove DBP precursors in the most cost and energy-effective manner.

To further improve upon our understanding of DBP precursors in FBW and to provide insight leading to the development of efficient removal strategies for precursors, we investigated the molecular composition of DOM by FT-ICR-MS in FBW samples collected from 10 DWTPs in Shanghai, China. To better understand the reactivity of DOM with free chlorine, the transformation of molecular formulae in FBW after chlorination was also investigated.

2. Materials and methods

2.1. Sample collection

FBW samples were collected from the overflow of gravity thickeners treating sand FBW at 10 DWTPs in Shanghai, China. Each plant consisted of conventional treatment processes (including coagulation, sedimentation, filtration, disinfection) and three treatment plants (#3, #4, and #10) also had ozone/biologically activated carbon (O₃/BAC) after the sand filters. Samples from treatment plants with O₃/BAC (#3, #4, and #10) were also collected from the gravity thickeners treating FBW (prior to O₃/BAC), and thus the treatment processes for all samples were similar/the same. The water sources were the Yangtze and Huangpu Rivers. All FBW samples were filtered by a 0.45 µm glass fiber filters and were then stored at 4 °C in refrigerators.

2.2. Chemical reagents

Pure DBP standards including four THMs, nine HAAs, six HAMS, and seven HANs purchased from Dr. Ehrenstorfer (Augsburg, Germany), and the detailed category and information are listed in Table S1. Other reagents, including hydrochloric acid, methyl tert-butyl ether, methanol, ultrapure water, etc., are described in the Supplementary material.

2.3. Formation potential experiments and analytical methods

Water samples were adjusted to pH 7 by 20 mM phosphate buffer solution and were then chlorinated at 25 °C in the dark for 72 h. The chlorine dose was calculated by Eq. (1). Excess sodium thiosulfate was used to quench residual chlorine after 72 h. All experiments were conducted in triplicate.

$$Cl_2 \text{ dose (mg/L)} = 3 \times DOC \text{ (mgC/L)} + 7.6 \times NH_3 \text{ (mgN/L)} + 10 \quad (1)$$

DBP were analyzed by the modified liquid-liquid extraction and gas chromatography, and the detailed methods are described in our previously publication (Qian et al., 2021) and in the Supplementary material. Bromide was measured by ion chromatography (ICS 600, Thermo Fisher Scientific, USA). UV absorbance at 254 nm (UV₂₅₄) and free chlorine were analyzed using a spectrophotometer (DR6000, HACH, USA) (APHA, 2005). A TOC analyzer (Multi N/C 2100, Analytik Jena AG, Germany) was used to measure DOC concentration. Dissolved organic carbon (DOC), UV₂₅₄, turbidity, pH, and bromide are provided in Table S3.

2.4. Molecular weight fractionation

The MW fractionation tests of each FBW samples were performed according to our previous publications (An et al., 2017; Qian et al., 2020) and in the Supplementary material. Briefly, FBW samples were fractionated by an ultrafiltration membrane (MW = 1 kDa). An aliquot of the <1 kDa filtrate was used to determine UV₂₅₄, DOC, DBPs, and DBP FPs. Another aliquot was used for FT-ICR-MS analysis. The value of UV₂₅₄ and concentrations of DOC, DBPs, and DBP FPs in the >1 kDa filtrate were calculated as the difference between the 0.45 µm filtrate and the <1 kDa filtrate.

2.5. FT-ICR-MS analysis

PPL cartridges were selected to extract 250 mL of each <1 kDa filtrate because it has been demonstrated to have high recoveries of DOM in various water matrices (Dittmar et al., 2008; Li et al., 2016). In our previously publication, we have described the pretreatment of water samples and FT-ICR-MS analysis in detail. Briefly, the water samples were extracted by PPL cartridges, and were then analyzed by FT-ICR-MS in ESI – mode (Sleighter and Hatcher, 2007). The Bruker DataAnalysis software and Matlab routines were used to analyze data and determine molecular formulae (Fu et al., 2020; Kellerman et al., 2014, 2018). The detailed information on the

pretreatment of water samples and FT-ICR-MS analysis methods are also provided in the Supplementary material. The relationship between DBP FPs and individual molecular formulae was assessed using Spearman rank correlation coefficients calculated by Python. Only molecular formulae coexisting in all water samples were investigated for correlation (X. Li et al., 2018; Zhang et al., 2019).

3. Results and discussion

3.1. DBP FP and precursor size fractionation

The total THM, HAA, HAM, and HAN FPs in the unfractionated samples were between 1063 and 2085, 124 and 259, 14 and 44, and 5 and 21 nM, respectively. TCM, DCAA, CAM, and DCAN were the most abundant species of THMs, HAAs, HAMs, and HANs, and accounted for 38–84 % of the total FPs of their respective groups on a molar basis (Fig. S2). The speciation towards more chlorinated species is reflective of the relatively low bromide concentrations in the samples ($\leq 95 \mu\text{g/L}$) and is consistent with the results from our previous research conducted on FBW (Qian et al., 2021).

To understand what fraction of the total precursors were amenable to high resolution mass spectrometry (i.e., low molecular weight), we measured the size distribution of the organic matter via sequential filtration, and each fraction's contribution to DBP FPs (McKenna et al., 2020). For all samples, >55 % of the total DOC was <1 kDa (the upper bound of the m/z measured in our experiments, Fig. S3). In Fig. 1 we show the contribution of each MW fraction to THM, HAA, HAN, HAM formation. For all water samples, the <1 kDa fraction contributed the greatest to the THM, HAA, HAN, and HAM formation, accounting for 56–89, 59–83, 56–75, and 53–91 % of the FPs in the unfractionated samples (molar basis). In our

previous research, we also found that low MW organic matter (<3 kDa) contained the majority of DBP precursors in FBW (Hu et al., 2021; Qian et al., 2020). Thus, the majority of DBP precursors were in the size range that is amenable to mass spectrometry.

3.2. Molecular distribution of DOM

We proceeded to measure and identify DOM in the fractionated samples (<1 kDa) via FT-ICR-MS. A representative mass spectrum is shown in Fig. S4. The molecular formulae of m/z in the range of 200–600 accounted for >83 % of the total molecular formulae and the median m/z was 393 Da to 427 Da. This is shown as kernel-based cumulative density plots (violin plots) in Fig. S5 and demonstrates that DOM in the 10 samples was similar in terms of MW distribution.

In terms of molecular formulae, >64 % and >76 % of the total formulae and their cumulative intensity, respectively, were attributable to compounds containing only CHO, CHON, and CHOCl, reflective of the relatively low incorporation of S into natural organic matter, even that which has been selectively removed and concentrated via filtration and gravity thickening (Fig. 2). Elements outside of C, H, O, N, S, and Cl, were not present in any formula because they were intentionally excluded during formula assignment (see Methods). Among these groups, CHO compounds had the greatest cumulative intensity (i.e., concentration), accounting for 34–46 % of the total ion current of mass peaks which were assigned a formula. Compounds containing only CHON were the most abundant in terms of number of formulae (i.e., molecular diversity), accounting for 29–32 % of the total formulae across the 10 treatment plants. The low cumulative intensity of N-containing compounds possibly because they could be difficultly ionized under negative ionization mode due to their

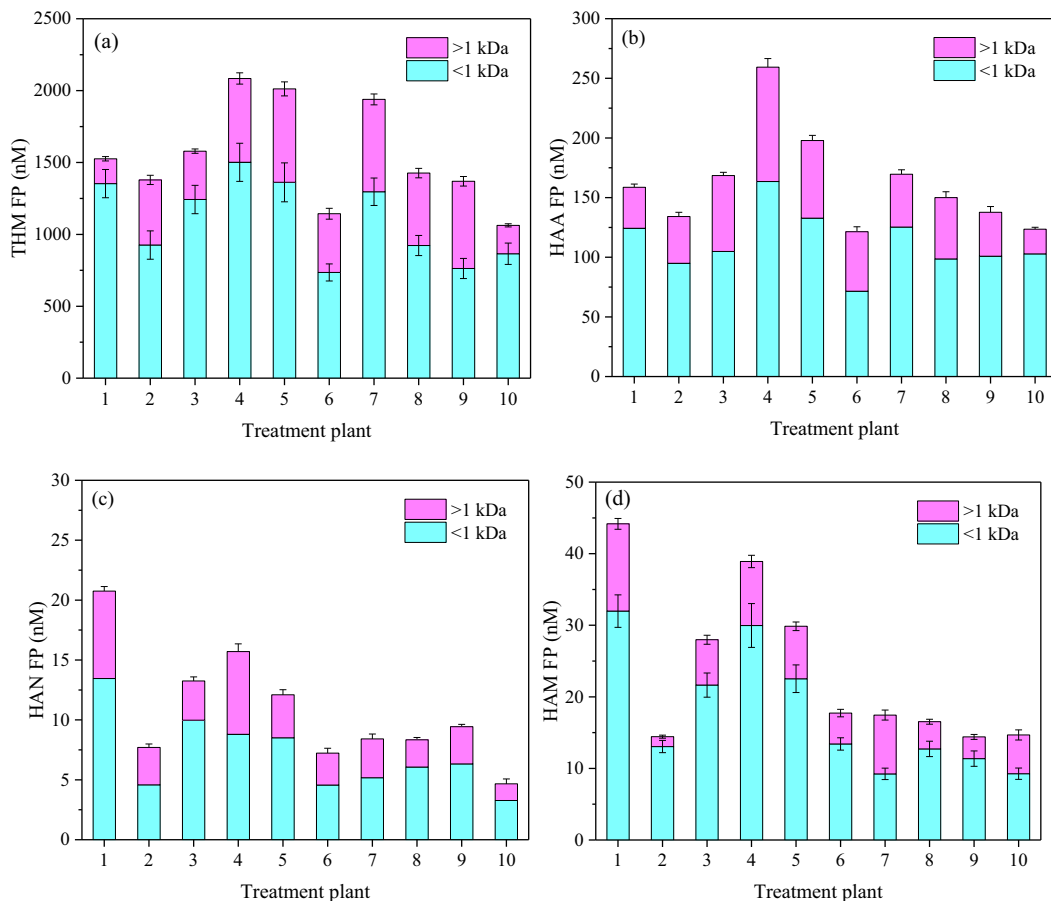


Fig. 1. (a) THM FP, (b) HAA FP, (c) HAN FP, and (d) HAM FP of two FBW MW fractionations from 10 DWTPs. Error bars represent one standard deviation ($n = 3$).

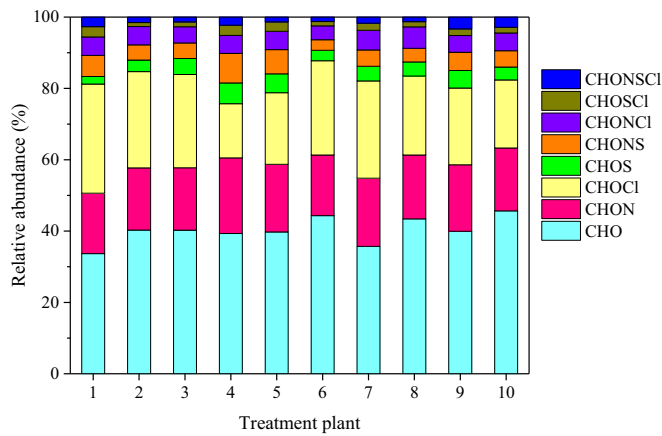


Fig. 2. Relative abundance of organic matter composition according to different formula classes.

high proton (Phungsai et al., 2016). Compounds containing chlorine accounted for 25–34 % of the total number of formulae. The large number of chlorine-containing formulae may have originated in the raw water, however, the backwash water was produced using finished water, which contained free chlorine residual, and thus a more likely explanation is that they were formed during backwashing.

Previous research has demonstrated strong correlation between DBPs and unsaturated DOM measured as double bond equivalents (DBE) (Farre et al., 2019; Stubbins et al., 2010; Wang et al., 2017; Zhang et al., 2019). Our recent study also showed that N-DBP formation was significantly correlated with the cumulative intensity of all CHON formulae with DBE > 10 ($R^2 = 0.79$ –0.89, $P < 0.05$) (Qian et al., 2022). In the FBW samples from the 10 treatment plants, the CHO and CHON intensity weighted DBE averages (DBE_{wa}) were much greater than the CHOCl DBE_{wa} (7.5–8.5 and 6.8–8.1 vs 4.1–6.8), indicating that CHO and CHON containing compounds were relatively unsaturated. Fig. S6 shows that there was a significant positive correlation ($R^2 = 0.72$ and 0.75, $P < 0.05$) between THM and HAA FPs and DBE_{wa} . HAN formation was also significantly correlated with the cumulative intensity of all CHON formulae with DBE > 10 (Fig. S7). These results suggest that highly unsaturated CHO- and CHON-containing compounds may have contributed to the formation of DBPs more than other compounds.

3.3. Transformation of DOM during chlorination

To understand the reactivity between groups of molecular formulae and chlorine, molecular formulae before and after chlorination were identified by FT-ICR-MS in the sample from treatment plant 3. This treatment plant was selected because the molecular composition (e.g., DBE, O/C, H/C, m/z) was near the median of all treatment plant samples (Table 1). Both before

Table 1

Elemental compositions of DOM in samples from 10 treatment plants prior to bench scale chlorination.

Treatment plant	Number of identified formulae	Cumulative intensity	m/z_{wa}	O/C _{wa}	H/C _{wa}	DBE _{wa}
1	6283	4.1×10^{11}	375.8	0.47	1.37	6.7
2	6822	3.6×10^{11}	370.4	0.46	1.42	6.4
3	7533	3.4×10^{11}	368.2	0.47	1.40	6.5
4	7925	3.2×10^{11}	403.4	0.49	1.39	7.2
5	8396	3.1×10^{11}	395.5	0.47	1.40	7.1
6	7184	4.0×10^{11}	361.2	0.46	1.40	6.4
7	8003	3.2×10^{11}	385.8	0.44	1.43	6.7
8	7280	3.7×10^{11}	368.5	0.47	1.38	6.7
9	8037	3.2×10^{11}	388.6	0.46	1.38	7.1
10	7095	3.7×10^{11}	377.5	0.48	1.38	6.9

and after chlorination, compounds containing only CHO, CHON, CHOCl, and CHONCl dominated, accounting for >78 % and >69 % of the total number of formulae and the cumulative intensity, and thus they are the focus of the discussion here. Notably, the sample prior to chlorination has a distribution among these groups that is also similar to the other treatment plant samples.

Chlorination decreased the DBE_{wa} from 7.6 to 6.2 for CHO-containing compounds and from 4.8 to 4.2 for CHOCl compounds (Table S8), likely owing to the chlorination of C=O and C=C double bonds (Ding et al., 2018; Gong et al., 2017). Contrarily, the DBE_{wa} of CHON and CHONCl compounds was higher after chlorination than before (DBE_{wa} increased from 7.3 to 8.5 and from 4.6 to 5.9, respectively). The saturation of nitrogenous organic matter may have decreased after chlorination because some nitrogenous precursors formed N-DBPs, containing a large number of highly unsaturated C=O double bonds and C≡N triple bonds (Nihemaiti et al., 2017).

More than 60 % of the compounds containing only CHO or CHOCl were recalcitrant to free chlorine oxidation, being present in both the pre- and post-chlorination samples (Table S9). However, the total cumulative intensity of CHO and CHOCl decreased by 44 % and 38 %, respectively. For nitrogenous organic matter (i.e., CHON and CHONCl), >69 % of formulae that were present in the pre-chlorinated samples were transformed during chlorination, demonstrating that the nitrogenous organic matter was more reactive with chlorine than other DOM.

Using this method of analysis it is not possible to determine products from individual compounds, but some of the transformed organic matter likely formed known and measured N-DBPs. Outside of the C- and N-DBPs that were directly measured, an additional 707 and 175 newly formed CHOCl and CHONCl oxidation by-products were formed and were detected in the chlorinated water sample. We are unable to measure their concentrations because of the inability to conclusively determine their structure, and because of the likely lack of analytical standards. However, at least one previous study demonstrated that the unknown fraction of total organic halogens is 50–60 % (Richardson et al., 2008). In this experiment, the unknown fraction contained newly formed (post-chlorination) compounds that accounted for 48 % of the total cumulative intensity. Therefore, the newly formed chlorine-containing compounds may account for 24–29 % of total organic halogens in FBW.

CHO, CHON, CHOCl, and CHONCl compounds which were transformed or newly formed during chlorination are shown in Kendrick mass defect (KMD) plots on a CH_2 scale in Fig. 3. The compounds which were removed by reactions with chlorine (no longer present in the mass spectra) tended to have lower KMD (intensity weighted KMD average (KMD_{wa}) of CHO, CHOCl, and CHONCl are presented in Table S10), and the newly formed compounds were distributed at higher KMDs. The KMD_{wa} of CHON was unchanged. Lower KMD generally indicates more hydrogen poor (e.g., aromatic compounds) and more oxygen rich molecules (Hughey et al., 2001; Sleighter and Hatcher, 2011). Together with the analysis of changes to DBE (i.e., decreasing DBE after chlorination) these data suggest that less saturated compounds preferentially reacted with chlorine to form byproducts.

For CHOCl and CHONCl compounds, the increased KMD of newly formed molecules compared to the pre-chlorinated samples suggests the substitution of halogens into the molecular structure. Increasing Cl/C ratio of newly formed molecules compared to the pre-chlorinated samples also supports this conclusion (Table S11). Below 200 Da, removed compounds begin to dominate the KMD plot. This is most likely due to some compounds being oxidized to lower MW structures which are outside the instrument m/z range rather than true removal of this DOM.

3.4. Linking DBP FP to individual compounds

We investigated the relationships between DBP FPs and individual molecular formulae which coexisted across all samples from the treatment plants to determine which subsets of the DOM pool are responsible for DBP formation. 2575 molecular formulae coexisted across the water

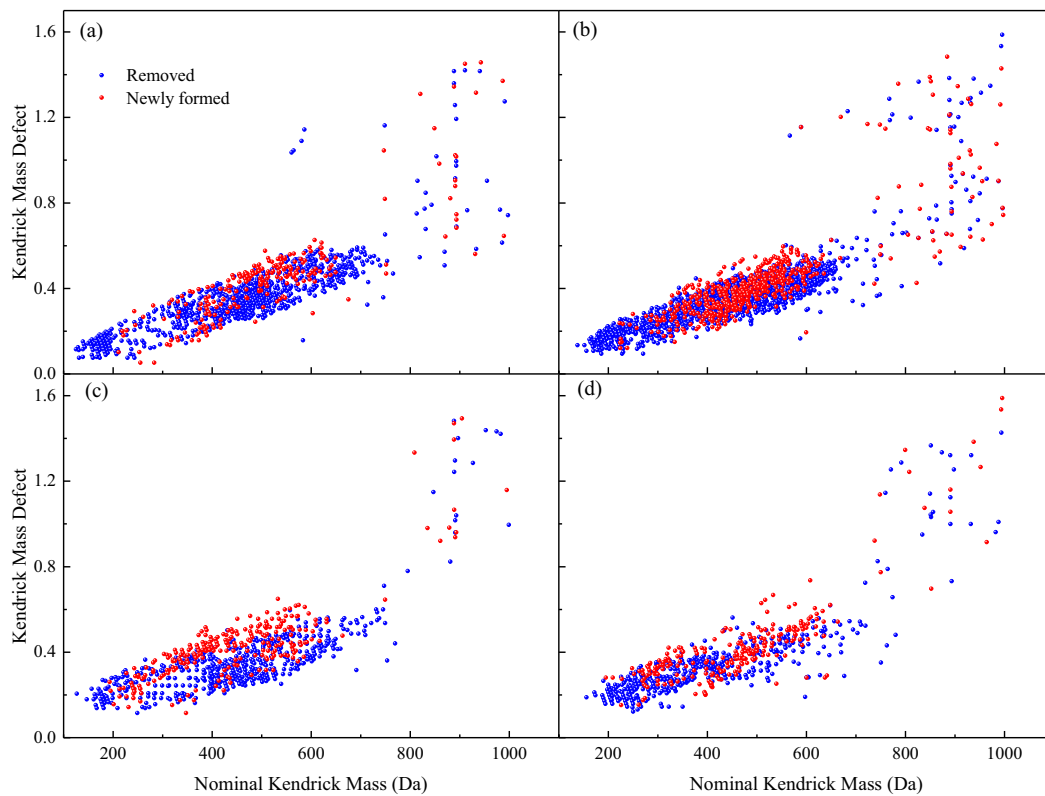


Fig. 3. KMD plots of (a) CHO, (b) CHON, (c) CHOCl, and (d) CHONCl formulae before and after chlorination. Removed formulae: present in the unchlorinated sample but not in the chlorinated sample. Newly formed formulae: present in the chlorinated sample but not the unchlorinated sample. Unchanged formulae: present in both the unchlorinated and chlorinated samples. Unchanged compounds are not shown.

samples among the >6000 formulae identified in each sample. Individual compounds and their correlation with DBP FPs are shown as van Krevelen plots in Fig. 4. 361, 142, 503, and 345 formulae were positively correlated (Spearman Rank order, $P < 0.05$) with THM FPs, HAA FPs, HAN FPs, and HAM FPs, respectively. Compounds that were most closely correlated with formation of THMs, HAAs, HANs, and HAMs tended to be aliphatic compounds (high H/C), and highly unsaturated and phenolic compounds (moderate H/C). Prior research has suggested that THM precursors in source water tend to have lower H/C ratios and greater O/C ratios than our research demonstrates (Wang et al., 2017). However, organic matter with low H/C and high O/C have been reported to be removed well by coagulation (Zhang et al., 2012) and therefore are unlikely to be present in these FBW samples. Sand filtration could preferentially remove the compounds containing high and moderate H/C and low O/C (e.g., H/C: 1.32, O/C: 0.43), which were then backwashed into FBW (Lavonen et al., 2015). This suggests a significant shift in the characteristics of precursors present in FBW compared to source water and indicates that treatment strategies imposed for removal of precursor material in the source water (e.g., enhanced coagulation) may not be effective for precursor from in-plant water recycling.

Comparisons to published literature regarding the molecular composition cannot be made for HAN and HAM precursors because no such data exists, but HAA precursors tended to be more highly unsaturated and phenolic compounds than aliphatic compounds when compared to other DBP precursors, which were broadly distributed among the two groupings. HAA precursors also had relatively high O/C ratios, which is consistent with a previous study that demonstrated that unsaturated aliphatic compounds are more prone to forming DCAA and TCAA (Wang et al., 2017). However, the finding that HAA precursors had H/C ratios typically >1.0 conflicts with the prior study. This is likely because the prior work was, again, conducted on source water samples, and the samples studied here

were from FBW. Thus, FBW is likely to enrich more saturated compounds, which are generally less reactive. This is supported by the reactivity of the DOC towards HAA formation (9.0–23.0 $\mu\text{gHAA}/\text{mgC}$ from these water treatment plants vs 70.5 $\mu\text{gHAA}/\text{mgC}$ in Wang et al., 2017), and provides evidence that FBW DOM is less prone to forming HAAs that influent organic matter. There were not other obvious trends in terms of O/C content, although there were fewer HAA precursors at O/C ratios of <0.2 than for THMs, HAAs, and HANs, indicative of greater O content of HAAs over other DBPs in this study and thus the demand for greater O content of the precursor.

For all groups of DBPs, the correlated formulae generally had MW of <450 Da (Fig. 4) consistent with prior reporting that low MW compounds tend to evade coagulation (Bond et al., 2010). While THM and HAA precursors were relatively broadly distributed below 400 m/z , HAM and HAN precursors fell into a tighter range of ~ 300 to 400 m/z (Fig. 4). Together, these results illustrate that aliphatic and highly unsaturated and phenolic compounds distributed in the relatively narrow molecular weight range of 300–450 Da can preferentially form HAMs during the chlorination of FBW. More effective removal strategies for low MW aliphatic compounds, and highly unsaturated and phenolic compounds may be required to mitigate the risk of FBW recycling or release to the environment.

3.5. Limitations

PPL cartridges were used to enrich and extract DOM because PPL cartridges have been shown to have high efficiency for DOM (Dittmar et al., 2008). However, some non-extractable DOM molecules may also contribute to DBP formation and are not part of this analysis. Furthermore, some DBP-reactive DOM might not be ionizable by ESI $-$, also leading to their lack of incorporation in the results. Therefore, the conclusions here are based on a subset of DOM rather than all DOM present in the initial samples.

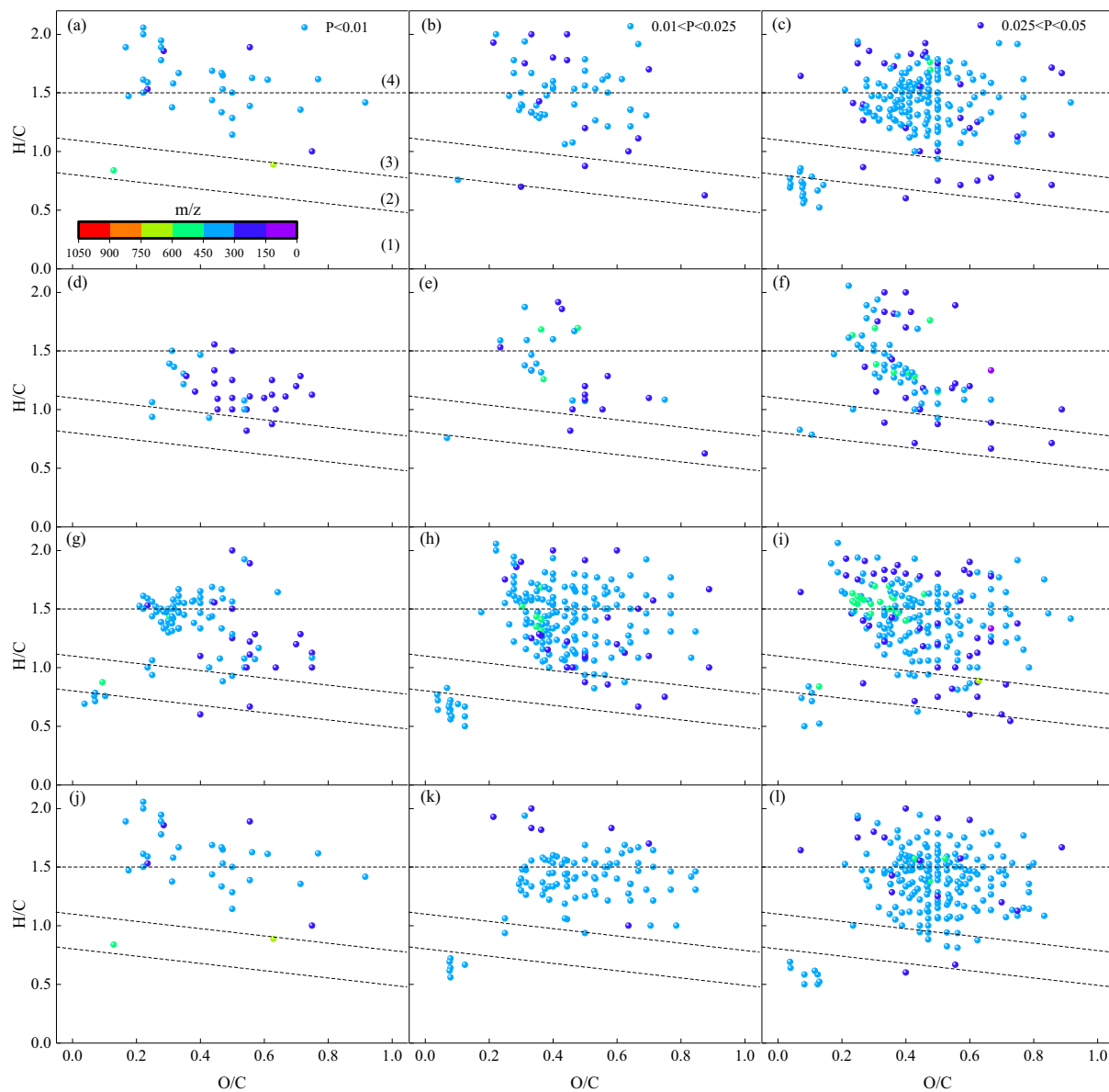


Fig. 4. Spearman's rank correlation between peak intensity of molecules/formulae existing in all 10 treatment plant FBW samples. (a–c) THM FP, (d–f) HAA FP, (g–i) HAN FP, and (j–l) HAM FP. (1) combustion-derived polycyclic aromatic, (2) vascular plant-derived polyphenols, (3) highly unsaturated and phenolic compounds, and (4) aliphatic compounds. P values decrease from left to right. MW is depicted as colors from red ($>900\text{ m/z}$) to purple ($<150\text{ m/z}$).

4. Conclusion

FBW contains DOM that increases the DBP-associated risk of source waters, either through in-plant recycling or release to the environment. We characterized the DOM present in FBW and found that low molecular weight aliphatic compounds and highly unsaturated and phenolic compounds were primarily responsible for the formation of THMs, HAAs, HAMs and HANs in FBW. Further, the reactive precursors tended to be lower in O/C ratios than prior reporting, except for HAAs, indicating broad changes to the DOM composition caused by coagulation/flocculation. Such a shift in DOM composition has implications for the treatment efficacy of existing infrastructure in removing DBP precursors contained in recycled FBW or FBW present in the source water. For example, lower O content precursors are potentially more difficult to remove by coagulation due to the reduced number of polar and ionic groups. FBW precursors also tended to be selectively enriched at lower MW ranges than would be expected for naturally occurring organic matter, again pointing to greater difficulty in removal via coagulation. This work, in combination with others which have studied the relationships

between DOM characteristics and DBP formation, provide the initial steps needed to understand the risk and potential treatment strategies for DOM contained in FBW. Given a better understanding of the impact of DOM characteristics on DBP formation, DWTPs may be able to determine treatment strategies that mitigate the risk of FBW recycling and from short- and long-term DOM changes in the watershed. In combination with future research the results may be extended to DBP forecasting after events which cause known impacts to drinking water treatment source waters. An example of such is wildfire, which mobilizes organic carbon that is relatively oxidized.

CRediT authorship contribution statement

Yunkun Qian: Conceptualization, Methodology, Investigation, Writing – original draft, Visualization. **Yijun Shi:** Validation, Data curation. **Jun Guo:** Formal analysis. **Yanan Chen:** Investigation, Data curation. **David Hanigan:** Writing – review & editing, Funding acquisition. **Dong An:** Conceptualization, Resources, Supervision, Project administration, Funding acquisition.

Data availability

Data will be made available on request.

Declaration of competing interest

The authors declare that they have no known competing financial interests or personal relationships that could have appeared to influence the work reported in this paper.

Acknowledgements

This research is supported by the National Natural Science Foundation of China (NSFC 22076026, 21777031, 21577024) and partially by the National Science Foundation (CBET-1804255).

Appendix A. Supplementary data

Supplementary data to this article can be found online at <https://doi.org/10.1016/j.scitotenv.2022.159027>.

References

An, D., Gu, B., Sun, S., Zhang, H., Chen, Y., Zhu, H., Shi, J., Tong, J., 2017. Relationship between THMs/NDMA formation potential and molecular weight of organic compounds for source and treated water in Shanghai, China. *Sci. Total Environ.* 605–606, 1–8.

APHA Water Environment Federation, A., 2005. *Standard Methods for the Examination of Water and Wastewater*. Twenty-First ed. APHA, Washington DC, USA.

Baldassarre, G.D., Wanders, N., AghaKouchak, A., Kuil, L., Rangecroft, S., Veldkamp, T., Garcia, M., van Oel, P.R., Breinl, K., Van Loon, A.F., 2018. Water shortages worsened by reservoir effects. *Nat. Sustain.* 1 (11), 617–622.

Bond, T., Goslan, E.H., Parsons, S.A., Jefferson, B., 2010. Disinfection by-product formation of natural organic matter surrogates and treatment by coagulation, MIEX and nanofiltration. *Water Res.* 44, 1645–1653.

Chen, H., Tsai, K.P., Liu, Y., Toli, N., Burton, S.D., Chu, R., Karanfil, T., Chow, A.T., 2020. Characterization of dissolved organic matter from wildfire-induced *Microcystis aeruginosa* blooms controlled by copper sulfate as disinfection byproduct precursors using APPI(-) and ESI(-) FT-ICR MS. *Water Res.* 189, 116640.

Chuang, Y., Szczuka, A., Mitch, W.A., 2019. Comparison of toxicity-weighted disinfection byproduct concentrations in potable reuse waters and conventional drinking waters as a new approach to assessing the quality of advanced treatment train waters. *Environ. Sci. Technol.* 53, 3729–3738.

Ding, S., Chu, W., Bond, T., Cao, Z., Xu, B., Gao, N., 2018. Contribution of amide-based coagulant polyacrylamide as precursors of haloacetamides and other disinfection by-products. *Chem. Eng. J.* 350, 356–363.

Dittmar, T., Koch, B.P., Hertkorn, N., Kattner, G., 2008. A simple and efficient method for the solid-phase extraction of dissolved organic matter (SPE-DOM) from seawater. *Limnol. Oceanogr. Meth.* 6, 230–235.

Farre, M.J., Jaen-Gil, A., Hawkes, J., Petrovic, Mira, Catalan, N., 2019. Orbitrap molecular fingerprint of dissolved organic matter in natural waters and its relationship with NDMA formation potential. *Sci. Total Environ.* 670, 1019–1027.

Fu, Q., Fujii, M., Riedel, T., 2020. Development and comparison of formula assignment algorithms for ultrahigh-resolution mass spectra of natural organic matter. *Anal. Chim. Acta* 1125, 247–257.

Gong, T., Tao, Y., Zhang, X., Hu, S., Yin, J., Xian, Q., Ma, J., Xu, B., 2017. Transformation among aromatic iodinated disinfection byproducts in the presence of monochloramine: from monoiodophenol to triiodophenol and diiodonitrophenol. *Environ. Sci. Technol.* 51, 10562–10571.

Gottfried, A., Shepard, A.D., Hardiman, K., Walsh, M.E., 2008. Impact of recycling filter backwash water on organic removal in coagulation–sedimentation processes. *Water Res.* 42 (18), 4683–4691.

Hanigan, D., McKenna, E., Song, M., Thurman, E.M., Ferrer, I., Roback, S., Plumlee, M.H., 2022. Nitrosamine Precursors in Direct and Indirect Potable Reuse Water. Water Research foundation Final Report. Water Research Foundation, Denver, CO.

Hu, Y., Qian, Y., Chen, Y., Guo, J., Song, J., An, D., 2021. Characteristics of trihalomethane and haloacetic acid precursors in filter backwash and sedimentation sludge waters during drinking water treatment. *Sci. Total Environ.* 775, 145952.

Hughey, C.A., Hendrickson, C.L., Rodgers, R.P., Marshall, A.G., Qian, K., 2001. Kendrick mass defect spectrum: a compact visual analysis for ultrahigh-resolution broadband mass spectra. *Anal. Chem.* 73, 4676–4681.

Kellerman, A.M., Dittmar, T., Kothawala, D.N., Tranvik, L.J., 2014. Chemodiversity of dissolved organic matter in lakes driven by climate and hydrology. *Nat. Commun.* 5, 1–8.

Kellerman, A.M., Guillemette, F., Podgorski, D.C., Aiken, G.R., Butler, K.D., Spencer, R.G.M., 2018. Unifying concepts linking dissolved organic matter composition to persistence in aquatic ecosystems. *Environ. Sci. Technol.* 52, 2538–2548.

Krasner, S.W., Westerhoff, P., Mitch, W.A., Hanigan, D., McCurry, D.L., Von Gunten, U., 2018. Behavior of NDMA precursors at 21 full-scale water treatment facilities. *Environ. Sci. Water Res.* 4 (12), 1966–1978.

Kummu, M., Ward, P.J., Moel, H., Varis, O., 2010. Is physical water scarcity a new phenomenon? Global assessment of water shortage over the last two millennia. *Environ. Chem. Lett.* 5 (3), 034006.

Lavonen, E.E., Kothawala, D.N., Tranvik, L.J., Gonsior, M., Schmitt-Kopplin, P., Kohler, S.J., 2015. Tracking changes in the optical properties and molecular composition of dissolved organic matter during drinking water production. *Water Res.* 85, 286–294.

Li, L., Xu, G., Xing, J., 2018a. Diatomite enhanced dynamic membrane technology for simultaneous backwash sludge pre-dewatering and backwash wastewater recycling. *J. Clean. Prod.* 211, 1420–1426.

Li, X., Sun, G., Chen, S., Fang, Z., Yuan, H., Shi, Q., Zhu, Y., 2018b. Molecular chemodiversity of dissolved organic matter in paddy soils. *Environ. Sci. Technol.* 52 (3), 963–971.

Li, Y., Harr, M., Lucio, M., Kanawati, B., Smirnov, K., Flerus, R., Koch, B.P., Schmitt-Kopplin, P., Hertkorn, N., 2016. Proposed guidelines for solid phase extraction of Suwannee River dissolved organic matter. *Anal. Chem.* 88 (13), 6680–6688.

Maizel, A.C., Li, J., Remucal, C.K., 2017. Relationships between dissolved organic matter composition and photochemistry in lakes of diverse trophic status. *Environ. Sci. Technol.* 51 (17), 9624–9632.

McKenna, E., Sharma, P., McCurry, D.L., Hanigan, D., 2020. A Layman's guide to high-resolution mass spectrometry. *J. Am. Water Work Assoc.* 112 (4), 40–49.

Nihemaiti, M., Roux, J.L., Hoppe-Jones, C., Reckhow, D.A., Croue, J.P., 2017. Formation of haloacetonitriles, haloacetamides, and nitrogenous heterocyclic byproducts by chloramination of phenolic compounds. *Environ. Sci. Technol.* 51 (1), 655–663.

Phungsa, P., Kurisu, F., Kasuga, I., Furumai, H., 2016. Molecular characterization of low molecular weight dissolved organic matter in water reclamation processes using Orbitrap mass spectrometry. *Water Res.* 100, 526–536.

Plewa, M.J., Kargalioglu, Y., Vanker, D., Minear, R.A., Wagner, E.D., 2002. Mammalian cell cytotoxicity and genotoxicity analysis of drinking water disinfection by-products. *Environ. Mol. Mutagen.* 40, 134–142.

Plewa, M.J., Muellner, M.G., Richardson, S.D., Fasano, F., Buettner, K.M., Woo, Y.T., McKague, A.B., Wagner, E.D., 2008. Occurrence, synthesis, and mammalian cell cytotoxicity and genotoxicity of haloacetamides: an emerging class of nitrogenous drinking water disinfection byproducts. *Environ. Sci. Technol.* 42 (3), 955–961.

Plewa, M.J., Simmons, J.E., Richardson, S.D., Wagner, E.D., 2010. Mammalian cell cytotoxicity and genotoxicity of the haloacetic acids, a major class of drinking water disinfection by-products. *Environ. Mol. Mutagen.* 51, 871–878.

Qian, Y., Chen, Y., Hu, Y., Hanigan, D., Westerhoff, P., An, D., 2021. Formation and control of C- and N-DBPs during disinfection of filter backwash and sedimentation sludge water in drinking water treatment. *Water Res.* 194, 116964.

Qian, Y., Chen, Y., Hanigan, D., Shi, Y., Sun, S., Hu, Y., An, D., 2022. pH adjustment improves the removal of disinfection byproduct precursors from sedimentation sludge water. *Resour. Conserv. Recycl.* 179, 106135.

Qian, Y., Hu, Y., Chen, Y., An, D., Westerhoff, P., Hanigan, D., Chu, W., 2020. Haloacetonitriles and haloacetamides precursors in filter backwash and sedimentation sludge water during drinking water treatment. *Water Res.* 186, 116346.

Richardson, S.D., Plewa, M.J., Wagner, E.D., Schoeny, R., DeMarini, D.M., 2007. Occurrence, genotoxicity, and carcinogenicity of emerging disinfection by-products in drinking water: a review and roadmap for research. *Mutat. Res.* 636, 178–242.

Richardson, S.D., Thruston, A.D., Krasner, S.W., Weinberg, H.S., Miltner, R.J., Schenck, K.M., Simmons, J.E., 2008. Integrated disinfection by-products mixtures research: comprehensive characterization of water concentrates prepared from chlorinated and ozonated/postchlorinated drinking water. *J. Toxicol. Environ. Health Part A* 71 (17), 1165–1186.

Sanchis, J., Jaen-Gil, A., Gago-Ferrero, P., Munthali, E., Farr, M.J., 2020. Characterization of organic matter by HRMS in surface waters: effects of chlorination on molecular fingerprints and correlation with DBP formation potential. *Water Res.* 176 (24), 115743.

Sanchis, J., Petrović, M., Farré, M.J., 2021. Prediction of NDMA formation potential using non-target analysis data: a proof of concept. *Environ. Sci.: Water Res. Technol.* 7, 2255–2267.

Shafiquzzaman, M., Al-Mahmud, A., AlSaleem, S.S., Haider, H., 2018. Application of a low cost ceramic filter for recycling sand filter backwash water. *Water (Basel)* 10 (2), 150–165.

Sleighter, R.L., Hatcher, P.G., 2007. The application of electrospray ionization coupled to ultrahigh resolution mass spectrometry for the molecular characterization of natural organic matter. *J. Mass Spectrom.* 42 (5), 559–574.

Sleighter, R.L., Hatcher, P.G., 2011. Fourier transform mass spectrometry for the molecular level characterization of natural organic matter: instrument capabilities, applications, and limitations. *Fourier Transforms—Approach to Scientific Principles*, pp. 295–320.

Smith, D.F., Podgorski, D.C., Rodgers, R.P., Blakney, G.T., Hendrickson, C.L., 2018. 21 Tesla FT-ICR mass spectrometer for ultrahigh-resolution analysis of complex organic mixtures. *Anal. Chem.* 90 (3), 2041–2047.

Spencer, R.G.M., Guo, W., Raymond, P.A., Dittmar, T., Hood, E., Fellman, J., Stubbins, A., 2014. Source and biolability of ancient dissolved organic matter in glacier and lake ecosystems on the Tibetan Plateau. *Geochim. Cosmochim. Acta* 142, 64–74.

Stubbins, A., Spencer, R.G.M., Chen, H., Hatcher, P.G., Mopper, K., Hernes, P.J., Mwamba, V.L., Mangangu, A.M., Wabakanghanzi, J.N., Six, J., 2010. Illuminated darkness: molecular signatures of congo river dissolved organic matter and its photochemical alteration as revealed by ultrahigh precision mass spectrometry. *Limnol. Oceanogr.* 55 (4), 1467–1477.

Szczuka, A., Parker, K.M., Harvey, C., Hayes, E., Vengosh, A., Mitch, W.A., 2017. Regulated and unregulated halogenated disinfection byproduct formation from chlorination of saline groundwater. *Water Res.* 122, 633–644.

Wagner, R., Plewa, M.J., 2017. CHO cell cytotoxicity and genotoxicity analyses of disinfection by-products: an updated review. *J. Environ. Sci.* 58, 64–76.

Walsh, M.E., Gagnon, G., Alam, Z., Andrews, R.C., 2008. Biostability and disinfectant by-product formation in drinking water blended with UF-treated filter backwash water. *Water Res.* 42 (8–9), 2135–2145.

Wang, X., Zhang, H., Zhang, Y., Shi, Q., Wang, J., Yu, J., Yang, M., 2017. New insights into trihalomethane and haloacetic acid formation potentials: correlation with the molecular composition of natural organic matter in source water. *Environ. Sci. Technol.* 51 (4), 2015–2021.

Yang, C., Yeh, C.H., Ho, C.C., 2015. Systematic quantitative risk analysis of water shortage mitigation projects considering climate change. *Water Resour. Manag.* 29 (4), 1067–1081.

Zhang, B., Shan, C., Hao, Z., Liu, J., Wu, B., Pan, B., 2019. Transformation of dissolved organic matter during full-scale treatment of integrated chemical wastewater: molecular composition correlated with spectral indexes and acute toxicity. *Water Res.* 157, 472–482.

Zhang, H., Zhang, Y., Shi, Q., Ren, S., Yu, J., Ji, F., Luo, W., Yang, M., 2012. Characterization of low molecular weight dissolved natural organic matter along the treatment train of a waterworks using fourier transform ion cyclotron resonance mass spectrometry. *Water Res.* 46 (16), 5197–5204.